A Photocatalysis of CV Dye Under UV Light Degradation using Laboratory Prepared In(OH)$_3$ And In$_2$O$_3$ By Hydrothermal Method: Nano-Matrrials For Dye Sensitive Solar Cell

Muktikanta Panigrahi [a, *], Adiraj Behera [b], Ratan Indu Ganguly [c], Radha Raman Dash [d]

[a] Department of Materials Science, Maharaja Sriram Chandra Bhanja Deo University, Baripada, Odisha-757003, India

[b] Department of Metallurgical and Materials Engineering, Government College of Engineering, Keonjhar, Odisha-758002, India

[c] Department of Metallurgical Engineering, National Institute of Technology, Raurkela, Odisha-769008, India

[d] National Metallurgical Laboratory, Jamshedpur, Jharkhand-831001, India

*Corresponding Author Email: muktikanta2@gmail.com

Abstract: Hollow microcubes with nanorods of Indium oxide (In$_2$O$_3$) are synthesized using hydrothermal followed by decomposition process. Synthesized materials are characterized with XRD, SEM, and FTIR spectroscopy for esteeming phase compositions and morphologies. The photocatalytic performances of two materials are evaluated by the degradation of crystal violet dye in an aqueous solution under UV light. The photocatalytic activity of prepared In(OH)$_3$ shows ~60% degradation of crystal violet after 5 h reaction, whereas In$_2$O$_3$ shows ~92% degradation under same conditions.

Keywords: In$_2$O$_3$, Crystal Violet Dye, Krikendal Effect, XRD, SEM, UV Visible, Photocatalysis

1. Introduction

Non-biodegradable pollutants in air and water are eliminated by using some semiconductors [1-7]. Usually, oxide semiconductors have higher band gap (5.5 eV). By UV light irradiation, electrons from adjourning areas are removed thereby, creating holes. Removed electrons have sufficient energy to overcome energy gap and cause conduction in materials. Enhanced properties of these materials are therefore, utilized for modern electronic applications [8].

Research scientists are taken interest to purify hazardous water near the dye industries and textile industries. In those areas, the effluent contains hazardous and toxic material that threatens the ecosystem by polluting the drinking water. If the dye's effluent is mixed with clean drinking water resources, it will cause odder and turbidity making it unsuitable for consumption. The colored water also affects the sea creatures. Dyes, including CV dye, have serious harm to humans' health; it can irritate the skin and eyes and damage the brain, kidney, liver, and immune system. Furthermore, respiratory problems occur when inhaling effluent contaminants with dyes when they evaporate. CV is toxic to mammalian cells and can cause faintness, diarrhea, headache, vomiting, and long-term exposure that may cause cancer. So, our aim is to develop a catalyst to purify CV dye contaminated water. That water is used as drinking water by the peoples stayed near by the areas.

It is for this reason, Indium oxide and hydroxide are studied exhaustibly for their physico-chemical properties as well as for their potential applications in various electronic fields [1, 9].

In(OH)$_3$ is observed to be an useful photocatalyst used for the removal of benzenes as compared to other materials such as P$_2$O$_5$, TiO$_2$ [2-7, 10]. It has now been accepted that In$_2$O$_3$ would be a suitable semiconductor for application in gas sensor, transparent conductors, solar cells and solid-state application devices [11]. Further studies are thought to be necessary to find out photoelectron catalytic activity of In(OH)$_3$ and In$_2$O$_3$ cubic nano-particles.

At present, there are different techniques available to produce nanoparticles [12, 13]. They are chemical vapour deposition, hot injection technique, organic solution synthetic route, hydrothermal methods [13], etc. These methodologies are utilized to synthesize In(OH)$_3$ and In$_2$O$_3$ with various shapes such as hollow shaped nanorods, nano belts, nanowires, etc [14]. Reports are available where In(OH)$_3$ and In$_2$O$_3$ particles are synthesized as cubic nanoparticle. A mixed micro structure of microcubes with nanorods of these two materials need further be studied for optoelectronic behaviour of two materials.

In the present investigation, template free surfactant less in (OH)$_3$ microcubes with nanorods and hollow microcubes of In$_2$O$_3$ are successfully synthesized by hydrothermal method. The cost is minimized to produce the mix micro structures. Reproducibility is checked. Photocatalytic activity is tested.

2. Experimental Details

2.1 Synthesis of In (Oh)$_3$ And In$_2$o$_3$

Analytical grade of Indium (III) chloride 99.99 % purity, Sodium hydroxide are used for the preparation of In(OH)$_3$ and In$_2$O$_3$. at room temperature. 40 mL of distilled water is poured into 0.07 M (0.155 gm) of Indium (III) chloride and is stirred still a clear liquid is obtained. During stirring, 0.8 M (0.032 gm) of NaOH is added to the solution. 0.02 M (0.034 gm). Oxalic acid is also added simultaneously to the above liquid and stirring process continuous for 20 minutes. Resulting solution is now transferred to a stainless steel autoclave where it is heated at 180 ^{0}C, continuously for 30 hrs in a hot oven. The product, thus, obtained is collected, washed with distilled water and ethanol mixture for three times. This is followed by a drying process in an oven at 60 ^{0}C for 5 hrs. The final product is grinded in a motar to a very fine size. The product is characterized with XRD for confirmation of the formation of In(OH)$_2$. In(OH)$_2$ is finally calcined for 10 minutes at 500 ^{0}C in an air furnace. The calcined powder is characterized with XRD for confirmation of the formation of In$_2$O$_3$.

2.2 Characterizations

The surface morphology of as prepared In(OH)$_3$ and In$_2$O$_3$ are studied using a Zeiss EVO 60. The structur of the samples is studied using a PANalytical High Resolution XRD, PW 3040/60 operated at 40 kV and 30 mA using Cu Kα radiations. FTIR spectra of prepared samples are studied by using Burker Tensor 27. Further to investigate the photocatalytic activity of In(OH)$_3$ and In$_2$O$_3$ samples are characterized by using UV-visible absorption spectroscopy (PerkinElmer, Lambda 750).

3. Results and Discussion

3.1 Structure and Morphology of in (Oh)$_3$ And In$_2$o$_3$

Diffraction peaks shown in Figure. 1 (a and b) perfectly match with cubic In(OH)$_3$ and In$_2$O$_3$ crystal structures with lattice constants. Lattice constants are 0.797 nm, and 1.012 nm, respectively [**JCPDS** card no 01-085-1338 for In(OH)$_3$ and 00-006-0416 for In$_2$O$_3$]. Presence of no other lines indicates purity of the two phases. Sharp peaks from those XRD patterns indicate crystallinity of those two products.

Figures. 2(a and b) are superimposed FTIR spectra of In(OH)$_3$ and In$_2$O$_3$ compounds. Presence of absorption band at 3232 cm^{-1} corresponds to the O-H vibration [15]. Absorption bands at 3128 and 2253 cm^{-1} is attributed to the O-H bond due to the adsorption of water molecules [16]. The absorption bands at 501, 778, and 1155 cm^{-1} are assigned to In-OH deformation vibration [17]. The bands at 853 and 1060 cm^{-1} are assigned to (O-InO) stretching vibration. In In$_2$O$_3$, the peak at 3440 cm^{-1}, accompanying by a weak peak at 1629 cm^{-1}, are due to O−H stretching vibration (vO−H) from residual water in KBr discs for FTIR measurement. The peaks at 1128 and 1344 cm$^{−1}$ are attributed to typical O−H bending vibration (γO−H). The peak at 466 and 605 cm$^{−1}$ are attributed to In−O vibration [17].
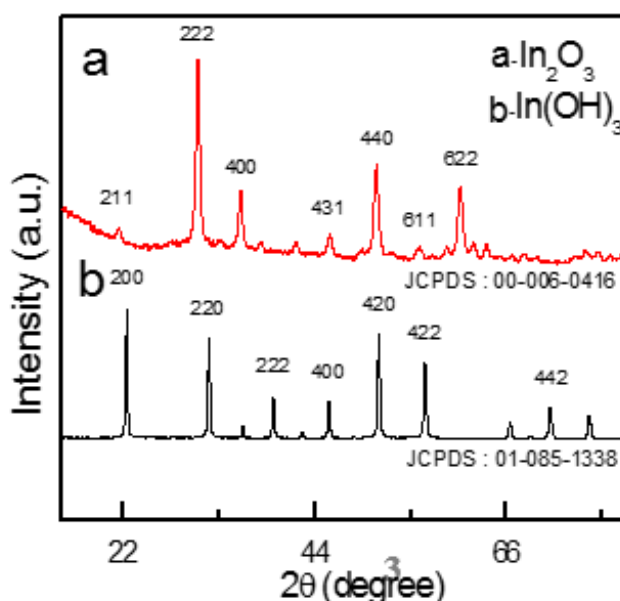

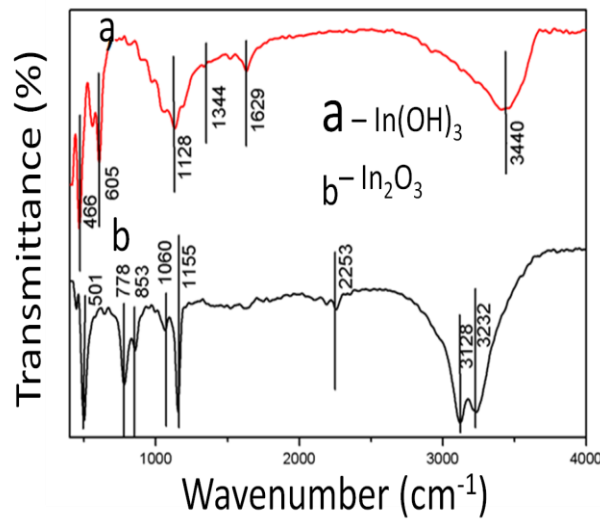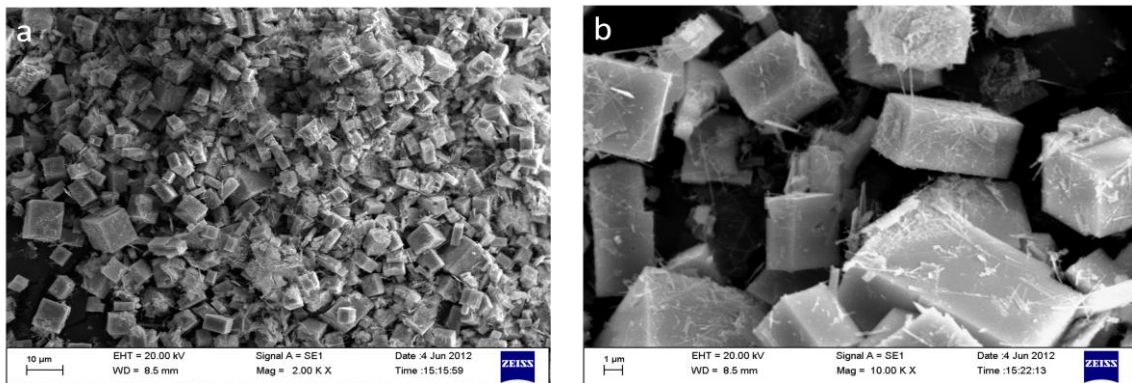**Figure 1.** XRD pattern of prepared (a) In$_2$O$_3$ and (b) In(OH)$_3$

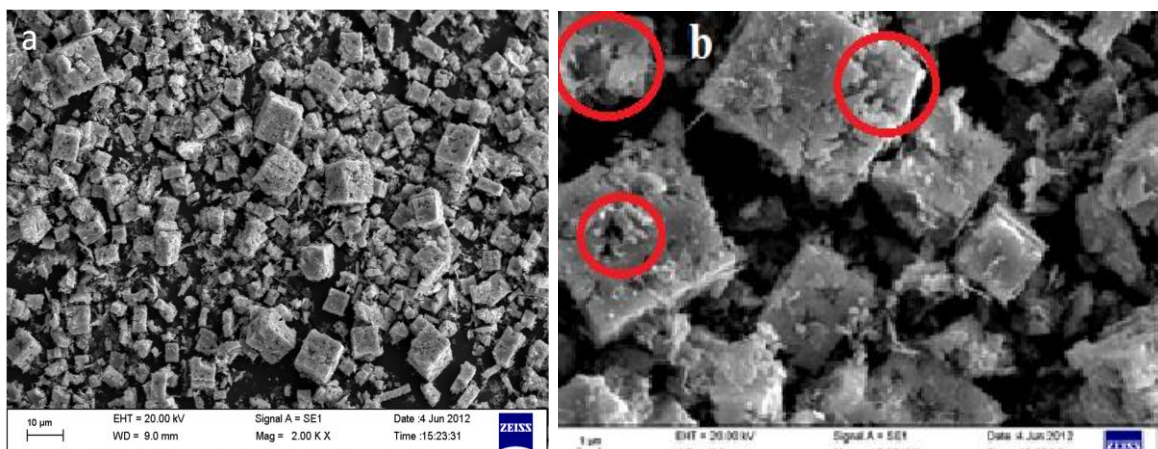**Figure 2.** FTIR spectra of In(OH)$_3$ and In$_2$O$_3$

a)   Low magnifing image   b)   high magnifying image

Figure 3. SEM image of In(OH)$_3$ microcubes with nanorods

a)   Low magnifying image   b)   high magnifying image

Figure 4. SEM image of In$_2$O$_3$ hollow microcubes with nanorods.

Figure 3a and 3b show the low- and high-magnification images of in $(OH)_3$ phase. In $(OH)_3$ shows solid microcubes and nanorods (Figure 3a).

Microstructures of In_2O_3 indicate hollow microcubes ranging between 1-5 micron with presence of nano rods less than 100 nm [Figure. 4 (a and b)]. Figure. 4 at different magnification (vide Figure. 4a and 4b). The sizes of microcubes are varying between 1-5 microns mixed with nanorods (size less than 100 nm). Marked positions in Figure 4b (higher magnification) are hollow in nature. Therefore, the microcubes are confirmed the hollow shapes. The hollow nature of In_2O_3 indicates a well-known phenomenon described as Krikendal effect [18].

The possible mechanism of formation In$(OH)_3$ solid microcubes and hollow microcubes of In_2O_3 with nanorods is thought to be in two stages. In the first stage, the in $(OH)_3$ solids are formed by hydrolysis of In^{3+} due to hydrothermal treatment at 200 °C. In the second stage, the in $(OH)_3$ gets transformed to In_2O_3 through decomposition. The Krikendal effect leads to Krikendal porosity *i.e.,* supersaturation of vacancies into hollow pores [19, 20]. Here, the anion exchange has occurred between OH^- of in $(OH)_3$ with O^{2-} of In_2O_3, leading to hollow structures rather than solid microcubes with nanorods.

3.2 Photocatalytic Activity

Photocatalytic properties of In$(OH)_3$ and In_2O_3 materials are evaluated by recording the extent of degradation occurred in crystal violet (CV) dye treated with 5×10^{-5} mol/L solution under UV light irradiation at $\lambda = 580$ nm. Figure.5a depicts UV-Visible spectra, indicating degradation of CV dye with In_2O_3 compounds.

Fig.5b shows a similar plot for In$(OH)_3$ compound. Plots are made for each material treated for different length of time. In each case, drop in peak height vis-à-vis decrease in areas under those curves with increase in the exposure time indicates the quantity of absorption occurred by the use of those crystalline materials. It is inferred that there substantial decrease in the peak heights for In_2O_3 if compared with In$(OH)_3$ compound i.e., 91 % for 5 h for In_2O_3 as compared to 60 % with In$(OH)_3$ compound peaks are formed between 500-600 nms. Thus, In_2O_3 is an efficient absorbent if compared with In$(OH)_3$ compound.

For our study, degradation time is 5 h which is efficient for the sample. At the degradation efficiency i.e. reducing degradation time may improve by preparing composite with in $(OH)2$ having band gap suited in visible region. This is our future study.

4. Conclusions

In$(OH)_3$ and In_2O_3 are successfully synthesized by using hydrothermal method. SEM micrographs show formation of microcubes and nanorods for both In$(OH)_3$ and In_2O_3. Porosity in In_2O_3 compound is believed to be due Krikendal effect *i.e.,* owing to migration of atoms in In$(OH)_3$ lattice during In_2O_3 transformation by calcination process. As a catalyst, In_2O_3 is found to be highly efficient for the degradation of crystal violet dye (~ 91 %) as compared to In$(OH)_3$ (~60 %) under UV Visible irradiation. Occurrence of peak is observed to be between 500-600 nm in UV spectra for both the materials of CV dye degradation. Higher degradation in In_2O_3 compound is due to higher surface area and lower band gap of the sample.
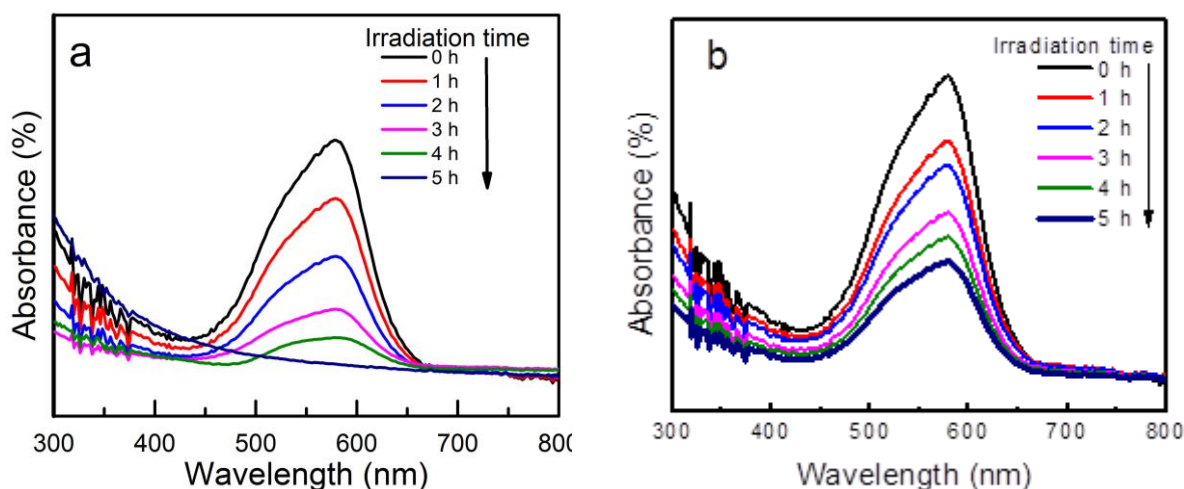

Figure 5. UV-vis spectra of CV dye degradation. (a) In_2O_3 (b) In$(OH)_3$.

References

[1] C. Shifu, Y. Xiaoling, Z. Huaye, L. Wei, Preparation, characterization and activity evaluation of heterostructure In2O3/In(OH)3 photocatalyst. Journal of Hazardous Materials, 180(1-3), (2010) 735-740. https://doi.org/10.1016/j.jhazmat.2010.04.108

[2] S. Tang, X. Zhang, S. Li, C. Zheng, H. Li, X. Xiao, rh-In2O3 Nanoparticles for Efficient Photocatalytic Degradation of Rifampin. ACS Omega, 8, (2023) 40099–40109. https://doi.org/10.1021/acsomega.3c02652

[3] S. Elbasuney, A.M. El Khawaga, M.A. Elsayed, A. Elsaidy, M.A. Correa Duarte, Enhanced photocatalytic and antibacterial activities of novel Ag-HA bioceramic nanocatalyst for waste-water treatment. Scientific Reports, 13, (2023) 13819. https://doi.org/10.1038/s41598-023-40970-4

[4] D.M. Tejashwini, H.V. Harini, H.P. Nagaswarupa, R. Naik, V.V. Deshmukh, N. Basavaraju, (2023), Review article An in-depth exploration of eco-friendly synthesis methods for metal oxide nanoparticles and their role in photocatalysis for industrial dye degradation. Chemical Physics Impact, 7, (2023) 100355. https://doi.org/10.1016/j.chphi.2023.100355

[5] F.T. Geldasa, M.A. Kebede, M.W. Shura, F.G. Hone, Experimental and computational study of metal oxide nanoparticles for the photocatalytic degradation of organic pollutants: a review. RSC Advanced, 13(27), (2023) 18404-18442. https://doi.org/10.1039/D3RA01505J

[6] A. Mancuso, N. Blangetti, O. Sacco, F.S. Freyria, B. Bonelli , S. Esposito, D. Sannino, V. Vaiano, Photocatalytic Degradation of Crystal Violet Dye under Visible Light by Fe-Doped TiO2 Prepared by Reverse-Micelle Sol–Gel Method, Nanomaterials, 13(2), (2023) 270. https://doi.org/10.3390/nano13020270

[7] S. Yan, X. Liang, S. Liu, Y. Zhang, J. Zeng, J. Bai, X. Zhu, J. Li, Synthesis of PANI@ α-Fe2O3/Al2O3 photo-Fenton composite for the enhanced efficient methylene blue removal. Journal of Sol-Gel Science and Technology, (2023) 1-13. https://doi.org/10.21203/rs.3.rs-3211246/v1

[8] S. Avivi, Y. Mastai, A. Gedanken, Sonohydrolysis of In3+ Ions: Formation of Needlelike Particles of Indium Hydroxide. Chemistry of Materials, 12(5), (2000) 1229-1233. https://doi.org/10.1021/cm9903677

[9] T. Yan, X. Wang, J. Long, P. Liu, X. Fu, G. Zhang, X. Fu, Urea-based hydrothermal growth, optical and photocatalytic properties of single-crystalline In(OH)3 nanocubes. Journal of Colloid Interface Science, 325(2), (2008) 425-431. https://doi.org/10.1016/j.jcis.2008.05.065

[10] Y.D. Zhang, Z. Zheng, F.L. Yang, Highly Sensitive and Selective Alcohol Sensors based on Ag-Doped In2O3 Coating. Industrial & Engineering Chemistry Research, 49(8), (2010) 3539-3543. https://doi.org/10.1021/ie100197b

[11] N. Taleban, M.R. Nilforoushan, Comparative study of the structural, optical and photocatalytic properties of semiconductor metal oxides toward degradation of methylene blue. Thin Solid Films, 518(8), (2010) 2210-2215. https://doi.org/10.1016/j.tsf.2009.07.135

[12] Y. Fang, X. Wen, S. Yang, Hollow and Tin-Filled Nanotubes of Single-Crystalline in (OH)3 Grown by a Solution–Liquid–Solid–Solid Route. Angewandte Chemie International Edition, 45(28), (2006) 4655-4658. https://doi.org/10.1002/anie.200601024

[13] J.M. Sánchez-Silva A. Aguilar-Aguilar, G.J. Labrada-Delgado, E.G. Villabona-Leal, H.J. Ojeda-Galván, J.L. Sánchez-García, H. Collins-Martínez, M.V. López-Ramón, R. Ocampo-Pérez, Hydrothermal synthesis of a photocatalyst based on Byrsonima crassifolia and TiO2 for degradation of crystal violet by UV and visible radiation. Environmental Research, 231(3), (2023) 116280. https://doi.org/10.1016/j.envres.2023.116280

[14] Z.B. Zhuang, Q. Peng, J.F. Liu, X. Wang, Y.D. Li, Indium Hydroxides, Oxyhydroxides, and Oxides Nanocrystals Series, Inorganic Chemistry, 46(13), (2007) 5179-5187. https://doi.org/10.1021/ic061999f

[15] P.S. Kohli, M. Kumar, K.K. Raina, M.L. Singla, Mechanism for the formation of low aspect ratio of La (OH) 3 nanorods in aqueous solution: thermal and frequency dependent behavior. Journal of Materials Science: Materials in Electronics, 23, (2012) 2257-2263. https://doi.org/10.1007/s10854-012-0793-7

[16] W.H. Ho, S.K. Yen, Preparation and Characterization of Indium Oxide Film by Electrochemical Deposition, Thin Solid Films, 498(1-2), (2006) 80-84. https://doi.org/10.1016/j.tsf.2005.07.072

[17] J.M. Hollas, (2004) Modern Spectroscopy. John Wiley & Sons Ltd, West Sussex, England.

[18] A.A. El Mel, R. Nakamura, C. Bittencourt, The Kirkendall Effect and Nanoscience: hollow Nanospheres and Nanotubes. Brillstein Journal of Nanotechnology, 6, (2015) 1348-1361. https://doi.org/10.3762/bjnano.6.139

[19] Y. Son, Y. Son, M. Choi, M. Ko, S. Chae, N. Park, J. Cho, Hollow Silicon Nanostructures via the Kirkendall Effect. Nano Letter, 15(10), (2015) 6914-6918. https://doi.org/10.1021/acs.nanolett.5b02842

[20] H.J. Fan, M. Knez, R. Scholz, D. Hesse, K. Nielsch, M. Zacharias, U. Gösele, Influence of Surface Diffusion on the Formation of Hollow

Nanostructures Induced by the Kirkendall Effect: The Basic Concept. Nano Letter, 7(4), (2007) 993-997. https://doi.org/10.1021/nl070026p

Authors Contribution Statement

Muktikanta Panigrahi: Conceptualization, Methodology, Data curation, Formal analysis, Validation, Writing – original draft, Writing – review & editing, Adiraj Behera: Writing – review & editing, Ratan Indu Ganguly Writing – original draft, Writing – review & editing, Radha Raman Dash - Writing – original draft, Writing – review & editing. All the authors read and approved the final version of the manuscript.

Has this article screened for similarity?

Yes